Efflux pumps mediate changes to fundamental bacterial physiology via membrane potential

Emily E Whittle[1], Oluwatosin Orababa[1†], Alexander Osgerby[2], Sarah J Element[1], Jessica MA Blair[1]* and Tim W Overton[2]*

[1] Institute of Microbiology and Infection, College of Medical and Dental Sciences and [2]School of Chemical Engineering, University of Birmingham, Edgbaston, Birmingham, B15 2TT, UK

† Present address: School of Life Sciences, The University of Warwick, Coventry, CV4 7AL

* To whom correspondence should be addressed:

Jessica MA Blair: j.m.a.blair@bham.ac.uk

Tim W Overton: t.w.overton@bham.ac.uk

Abstract

Efflux pumps are well known to be an important mechanism for removing noxious substances such as antibiotics from bacteria. Given that many antibiotics function by accumulating inside bacteria, efflux pumps contribute to resistance. Efflux pump inactivation is a potential strategy to combat antimicrobial resistance, as bacteria would not be able to pump out antibiotics. We recently discovered that the impact of loss of efflux function is only apparent in actively growing cells. We demonstrated that the global transcriptome of *Salmonella* Typhimurium is drastically altered during slower growth leading to stationary phase cells having a re-modelled, less permeable, envelope that prevents antibiotics entering the cell. Here, we investigated the effects of deleting the major efflux pump of *Salmonella* Typhimurium, AcrB, on global gene transcription across growth. We revealed that an *acrB* knockout entered stationary phase later than the wild type strain SL1344, and displayed increased and prolonged expression of genes responsible for anaerobic energy metabolism. We devised a model linking efflux and membrane potential, whereby deactivation of AcrB prevents influx of protons across the inner membrane and thereby hyperpolarisation. Knockout or deactivation of AcrB was demonstrated to increase membrane potential. We propose that the global transcription regulator ArcBA senses changes to the redox state of the quinol pool (linked to the membrane potential of the bacterium) and coordinates the shift from exponential to stationary phase via the key

master regulators RpoS, Rsd, and Rmf. Inactivation of efflux pumps therefore influences the fundamental physiology of *Salmonella*, with likely impacts on multiple phenotypes.

Importance

We demonstrate for the first time that deactivation of efflux pumps brings about changes to gross bacterial physiology and metabolism. Rather than simply being a response to noxious substances, efflux pumps appear to play a key role in maintenance of membrane potential and thereby energy metabolism. This discovery suggests that efflux pump inhibition or inactivation might have unforeseen positive consequences on antibiotic activity. Given that stationary phase bacteria are more resistant to antibiotic uptake, late entry into stationary phase would prolong antibiotic accumulation by bacteria. Furthermore, membrane hyperpolarisation could result in increased generation of reactive species proposed to be important for the activity of some antibiotics. Finally, changes in gross physiology could also explain the decreased virulence of efflux mutants.

Keywords

Hyperpolarisation, RND efflux pump, AcrAB-TolC, ArcBA, redox state, energy metabolism.

Introduction

Many antibiotics function by accumulating inside bacteria and inhibiting essential metabolic functions such as protein synthesis, DNA repair, or cell wall synthesis (1). Bacteria can therefore protect themselves against these antibiotics by decreasing intracellular accumulation. There are two main mechanisms for this: removal of antibiotics from inside the cell via efflux pumps (2); and prevention of influx of antibiotics across the envelope (3). The major efflux pump in *S*. Typhimurium is AcrAB-TolC, a member of the RND family (4) comprising the transporter AcrB, the periplasmic adaptor protein AcrA, and the outer membrane channel TolC. AcrAB-TolC has been shown to have a wide substrate range and mediate resistance to multiple antibiotics. Loss of AcrB function through mutation or inhibition has been shown to make *S*. Typhimurium hyper-susceptible to antibiotics as well as avirulent, unable to form biofilm and less motile (5, 6); major changes to the physiology of the organism.

In an attempt to understand the physiological consequences of loss of efflux function previous studies have compared global gene expression in the *S.* Typhimurium wild type and efflux mutants (5–7).

Wang-Kan *et al*. compared an *acrB* D408A mutant (defective in AcrB efflux function) with the wild type *S.* Typhimurium SL1344, both in exponential phase growth in MOPS minimal medium (6) and stationary phase growth in rich LB broth (7). The latter study also compared gene expression in *E. coli* K-12 MG1655 and its *acrB* D408A mutant, and characterised the exometabolome and endometabolome of each of the four strains in order to better understand the substrates of the AcrAB-TolC pump. The effect of deletion of *acrD*, encoding an alternative efflux pump with narrower substrate specificity to AcrB, on global gene expression has also been characterised (8). However, each of these studies compared gene expression at a single timepoint.

In a previous study (9) we investigated the dynamic balance between efflux and prevention of influx of antibiotics across the Gram-negative bacteria and revealed that efflux is more important during rapid exponential phase growth as the envelope is more fluid and antibiotics can pass into the bacterium more readily. However, in stationary phase, the envelope is remodelled and becomes less amenable to antibiotic entry, thus preventing intracellular accumulation, meaning that efflux has less impact. We used RNA-Seq in *Salmonella* Typhimurium SL1344 to map global gene expression as bacteria transitioned from exponential to stationary phase, highlighting gene expression changes potentially responsible for remodelling multiple layers of the envelope. Work by others has also revealed that prevention of influx and active efflux have different relative contributions during antimicrobial resistance development across Gram-negative pathogens (10, 11).

Given that the relative impact of efflux varies during bacterial growth, in the present study, we tracked gene expression at 1, 3 and 5 hours growth in the wild type and an Δ*acrB* mutant to enable the dynamics of gene expression to be compared. We sought to better understand the physiological changes brought about by deletion of *acrB*, and to differentiate between the direct effects of AcrB as an efflux pump (eg removal of compounds from the bacterium) and the secondary effects brought about by the deletion.

We show that deletion of *acrB* has wide-ranging effects on physiology and we propose and test a model that links efflux, membrane potential, redox state of the cell, and entry into stationary phase. This suggests that efflux pumps are deeply embedded in bacterial physiology, and loss of AcrB function perturbs the transition from exponential phase to stationary phase physiology. We also demonstrate the benefits of transcriptome analysis across growth, using samples taken at multiple timepoints, to discover novel aspects of gene regulation and physiology.

93 **Results**

94 We previously published the results of a transcriptome analysis showing transition of the wild type *S.*
95 Typhimurium strain SL1344 from exponential to stationary phase (9). Samples were taken after 1, 3,
96 and 5 hours growth in MOPS minimal medium, and gene expression was tracked using RNA-Seq across
97 growth. This study revealed changes to aspects of physiology as bacteria transitioned from the rapid
98 growth of exponential phase to the slower growth of stationary phase. We specifically focused on
99 changes in gene expression responsible for remodelling the bacterial envelope from a relatively
100 permeable structure in rapid growth to a far less permeable state in stationary phase. This decreased
101 envelope permeability is likely a key contributor to why stationary phase bacteria are more resistant
102 to multiple antibiotics (12, 13) as well as other stressors (14, 15).

103 In the present work, we expanded this study by repeating these transcriptomics experiments in an *S.*
104 Typhimurium Δ*acrB* mutant (9), similarly taking samples after 1, 3, and 5 hours growth in MOPS
105 minimal medium. The two strains grew similarly under these conditions. First, we compared how
106 changes in gene expression over time differed between the wild type and Δ*acrB* strains. Gene
107 expression was compared between 1 h and 3 h, 1 h and 5 h, and 3 h and 5 h timepoints for each strain
108 (Figure 1). This revealed that more genes were differentially regulated early in growth (the 1 h vs 3 h
109 comparison) in the wild type than in the Δ*acrB* mutant. Comparing later timepoints, there are more
110 differentially expressed genes for the 3 h vs 5 h comparison in the Δ*acrB* mutant than the wild type.
111 This suggests that changes in gene expression occur later in the Δ*acrB* mutant than the wild type.

112

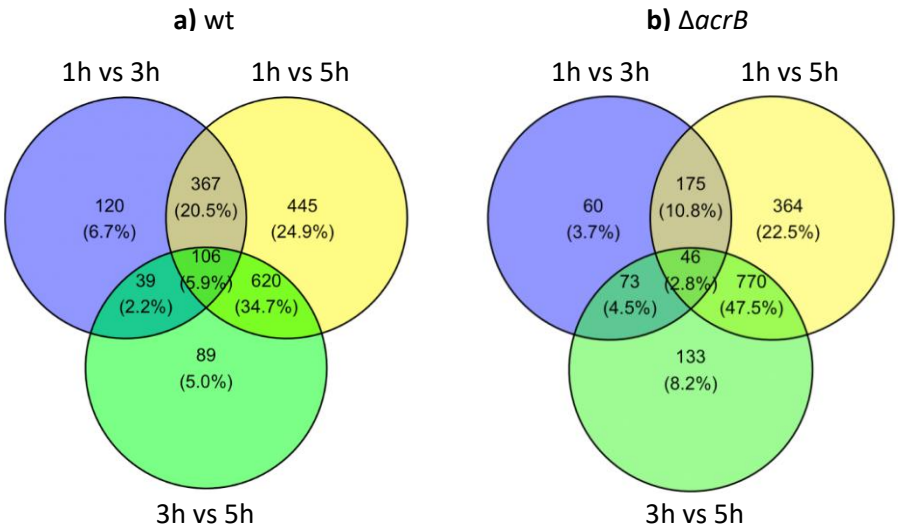

113 **Figure 1. Venn diagrams comparing gene expression in the (a) wild type and (b) Δ*acrB* strain.** Number of genes
114 differentially expressed ($\log_2$ foldchange ≥ 1.5 and $p_{adj} < 0.05$) for each comparison is shown.

115

116 We wanted to understand why expression of more genes changed between 1 h and 3 h in the wild
117 type than in the Δ*acrB* strain, and the effect this would have on physiology. We classified genes into
118 three groups (Figure 2) based on their log_2 fold change (log_2FC) from 1 h to 3 h in each strain, and their
119 Δlog_2FC value, calculated by subtracting the Δ*acrB* log_2FC from the wild type log_2FC. A positive Δlog_2FC
120 value denotes a gene that is more upregulated or less downregulated in the Δ*acrB* strain than the wild
121 type. Genes with a negative Δlog_2FC value are more upregulated or less downregulated in the wild
122 type.

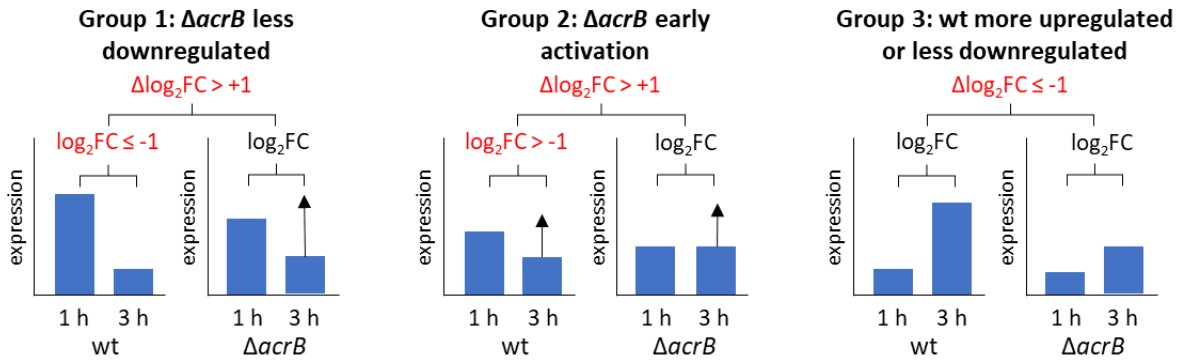

123

124 **Figure 2. Data analysis strategy to characterise differentially expressed genes.** For each gene, transcript levels
125 at 1 h and 3 h were compared and a log_2 fold-change (log_2FC) value calculated. The log_2 fold-change for the
126 Δ*acrB* mutant was subtracted from the wt log_2FC to give a Δlog_2FCvalue indicating the difference in regulation
127 between the two strains. A positive Δlog_2 value indicates a gene is more upregulated or less downregulated in
128 Δ*acrB* for the 1 h vs 3 h timepoints. A negative Δlog_2 value indicates that a gene is more upregulated or less
129 downregulated in the wild type.

130

131 Group 1 comprises genes that were downregulated from 1 h to 3 h in the WT ($log_2FC \leq -1$) and less
132 downregulated in the Δ*acrB* strain, thereby having a Δlog_2FC of ≥ 1. Group 2 contains genes that were
133 not downregulated from 1 h to 3 h in the wt ($log_2FC > -1$) but had a Δlog_2FC of ≥ 1, thereby were more
134 upregulated or less downregulated in the Δ*acrB* mutant. Group 3 contains genes that were more
135 upregulated from 1 h to 3 h in the wild type than in the Δ*acrB* mutant. Genes with a $p_{adj} > 0.05$ (non-
136 significant) for the 1 h to 3 h timepoints in either wt or Δ*acrB* were omitted from this analysis.

137 ***Group one – late repression in the ΔacrB strain***

138 The 166 genes in group one are more downregulated between 1 h and 3 h in the wild type than the
139 Δ*acrB* strain (Supplemental Table S1). The largest categories of genes in this group are those encoding
140 tRNAs (34 genes) and ribosomal proteins and other proteins involved in translation (33 genes). Many
141 of these genes (including the tRNA genes) are known to be downregulated during the entry into
142 stationary phase by the stringent response, mediated by ppGpp (16). For many of these genes,
143 expression is downregulated in the wild type from 1 h to 3 h and then does not change significantly

144 from 3 h to 5 h, whereas in the Δ*acrB* strain expression does not change from 1 h to 3 h but decreases
145 from 3 h to 5 h. This suggests that the Δ*acrB* strain enters stationary phase later than the wild type
146 SL1344 strain.

147 Fifteen genes in this group are involved in envelope functions including inner membrane protein
148 insertion, outer membrane lipoprotein trafficking, LPS and lipid A synthesis, and peptidoglycan
149 synthesis and remodelling. The peptidoglycan-related genes *ldtB*, *mrcA* and *pbpG* are implicated in
150 exponential phase functions (9, 17). Five genes involved in nucleotide metabolism and 6 genes in
151 amino acid metabolism, also important during rapid growth, are also in this group, reinforcing the idea
152 that stationary phase transition is delayed in the Δ*acrB* strain.

153 Four genes in group one are related to polyamines, specifically putrescine import and spermidine
154 synthesis. Recently, the efflux regulator AcrR (which represses expression of *acrAB*) was shown to bind
155 to three polyamines and regulate aspects of polyamine efflux and metabolism in *E. coli* (18). Seven
156 genes of *Salmonella* pathogenicity island 1 (SPI-1), encoding a type III secretion system required for
157 invasion of epithelial cells, are in group one. The SPI-1 regulatory network is very complex (19) and
158 comprises transcription factors encoded both within and outside SPI-1. Expression of SPI-1 is bistable
159 (20) and is influenced by multiple environmental stimuli including osmolarity, oxygen tension, bile,
160 [Mg^{2+}], and pH. Two genes in SPI-11, implicated in survival in the macrophage (21), are also in group
161 one. Alteration in SPI expression would likely influence virulence, which is known to be decreased
162 upon loss of AcrB function (6).

163 Other transcriptomic studies identified genes in group one being as being differentially regulated in
164 the *S.* Typhimurium wild type and strains lacking *acrB* or *acrB* function (*acrB* D408A mutant).
165 Comparison in exponential phase in MOPS minimal medium (5, 6) revealed that SPI-1 genes were
166 downregulated in an *acrB* knockout mutant and in the *acrB* D408A mutant. In stationary phase (7),
167 rRNAs, tRNAs, SPI-11 and some SPI-1 genes were downregulated (although the SPI-1 *sipABCD* TTSS
168 genes, not members of groups one-three in the present study, were upregulated in the mutant).
169 However, our data suggests that this is a response to fundamental changes in physiology brought
170 about by deletion of *acrB*, and not necessarily direct regulation of pathogenicity islands.

171 ***Group two – early activation in the ΔacrB strain***

172 The 46 genes in group two (Supplemental table S2) are more upregulated between 1 h and 3 h in the
173 *acrB* strain than in the same time period in the wild type, so are classified as "early activation". On
174 initial inspection, this group contains many genes known to be anaerobically activated. For each gene,
175 expression data in the gene expression database SalComMac (22, 23) was consulted to identify which

176 genes are anaerobically activated; in this database, “anaerobic shock” is classified as aerobic growth
177 followed by 30 minutes in a sealed static tube (22). It should be noted that the SalComMac data is for
178 *S*. Typhimurium strain 4/74; SL1344 is a *hisG* auxotroph of 4/74 (24), although we believe that data
179 should be broadly comparable for the two strains.

180 Many of the anaerobically-activated genes are activated by the oxygen-sensing global regulator FNR
181 in *Salmonella* (25) and / or *E. coli* (26). These include genes encoding the periplasmic nitrate and nitrite
182 reductases responsible for anaerobic respiration at low NO_2^- and NO_3^- concentrations (27, 28), the
183 anaerobic serine/threonine degradation enzyme TdcB that is suggested to be critical for energy
184 metabolism during changes in oxygen tension (29), and the two cytochrome *c* maturation (Ccm)
185 operons, one of which is downstream of the *nap* operon (30). The cytochrome *c* peroxidase *yhjA*/*ccp*
186 is also in this group, which has been shown to be FNR-activated (25) and enables respiratory growth
187 on peroxide (31). The *ccp* gene is upstream of the second *ccm* cluster and may form a single operon.
188 RS22105, annotated as a molybdopterin-dependent oxidoreductase and proposed to be a DMSO
189 reductase distinct from DmsABC, has been shown to be FNR activated in *Salmonella* (25), as has
190 *yhbU/ubiU* which encodes part of the oxygen-independent ubiquinone synthesis pathway (32).

191 A high affinity nickel uptake system (*yntABCDE/nikABCDE*) is in the grouping (33); these genes are FNR
192 activated in *E. coli* although were not identified in the *Salmonella* FNR study (25). In *E. coli*, *nikABCDE*
193 expression is linked to that of the Ni^{2+} cofactor-containing hydrogenases required for respiration of
194 fumarate and formate (34). RS15890 and RS15900 (*ecfT*) are two members of a putative 5-gene
195 operon encoding an ECF transporter suggested to import Co^{2+} (35) that is conserved in pathogenic *E.*
196 *coli* strains. SalComMac data suggests that this operon is anaerobically activated.

197 The remaining anaerobically-activated genes in this group are of unknown function or are poorly
198 characterised: *yecH* has been shown to be downregulated by adrenaline (36); *ompX* is in SPI-5 (37)
199 and has been found to be overexpressed in a *dksA* mutant (38); two LysR family transcriptional
200 regulators (RS11710 and RS19740); a putative transketolase RS12010; and hypothetical protein
201 RS12010.

202 It should be noted that for many of these anaerobic genes, expression increases from 1 h to 3 h and
203 then decreases from 3 h and to 5 h. The magnitude of the increase in expression is larger in the *acrB*
204 strain. Taken together, genes in this group enable anaerobic energy generation through respiratory
205 and substrate-level routes.

206 As well as the anaerobically-activated genes in this group, there are also several genes that are
207 anaerobically repressed in SalComMac, including the tyrosine importer *tyrP*, the flagellar genes *fliR*,

208 *fliF* and *fliH* and the proposed virulence factor *srfA* which was also identified as a class 2 flagellar gene
209 (39) whose expression is activated by the flagellar master regulator FlhDC. As previously noted, loss
210 of AcrB function reduces *Salmonella* motility (5). A link between motility and SPI-1 has also been
211 reported (40).

212 In previous transcriptomic studies, Wang-Kan et al (6) identified anaerobically-activated genes
213 including nitrate and nitrite reductase and flagellar genes being upregulated in the *acrB* D408A mutant
214 in exponential phase. In stationary phase, some anaerobically-relevant and flagellar genes were also
215 upregulated (7).

216 ***Group three – late activation in the ΔacrB strain***

217 Group three comprises 53 genes that are more activated in the wild type than in Δ*acrB* at three hours,
218 so the opposite pattern to genes in groups one and two (Supplemental Table S3). The most striking
219 group of genes in this group are the *met* genes involved in methionine biosynthesis from aspartate,
220 methionine uptake, and S-adenosyl methionine (SAM) biosynthesis; expression of these genes is seen
221 to "spike" at 3 h in the wt, with upregulation at 3 h vs 1 h and downregulation at 5 h vs 3 h. In the
222 Δ*acrB* strain these genes are less upregulated at 3 h and many are further upregulated at 5 h,
223 indicating much later induction. In *E. coli* these genes are all repressed by the regulator MetJ which
224 binds to methionine and SAM (41). Our data suggest that these routes to SAM are highly upregulated
225 on entry to stationary phase. SAM is an essential metabolite and a major methyl donor for protein and
226 DNA methylation and polyamine synthesis; in the transition to stationary phase, SAM is also a methyl
227 donor for cyclopropane fatty acid synthesis (42). In *E. coli*, the SAM synthase *metK* is essential (43) and
228 depletion of SAM using a *metK84* mutant leads to a cell division defect (44). In *S*. Typhimurium,
229 methionine biosynthesis or import are required for infection in mice and methionine was implicated
230 in aspects of peptidoglycan synthesis (45).

231 These data suggest that the methionine and / or SAM pool in the wild type is depleted at 3 h growth,
232 and these pathways are upregulated to replenish the pool. The transcriptomics data in SalComMac
233 shows that most of the *met* genes are not upregulated in stationary phase, although that dataset was
234 generated for cultures grown in rich Lennox broth (22). We suggest that in Lennox broth, methionine
235 is available (around 70 mg/L based on typical composition values (46)) so can be readily imported and
236 converted to SAM, whereas in MOPS minimal medium used here, methionine needs to be synthesised
237 from aspartate, hence activation of the *met* genes. This suggests that methionine could be a growth
238 limiting nutrient in these conditions.

239 A cluster of genes (*ybdL, ybdH, ybdD, ybdM*) are also regulated in a similar manner to the *met* genes.
240 *E. coli* YbdL has methionine aminotransferase activity (47) and is believed to be involved in methionine
241 recycling following polyamine synthesis (48). YbdH is annotated as a putative glycerol dehydrogenase
242 and the homologue in *E. coli* has been identified as a hydroxycarboxylate dehydrogenase (49). The *E.*
243 *coli ybdD* homologue has been identified (with CstA) as part of a pyruvate import system (50) and
244 *ybdM* has been identified as a transcriptional regulator related to SpoOJ (51). A predicted MetJ binding
245 site in this cluster could explain its regulation (41).

246 The PstSCAB high-affinity phosphate importer is poorly understood in *Salmonella* but is known to be
247 induced in *E. coli* in response to phosphate limitation, and is activated by RpoS (52). ProP is responsible
248 for the uptake of osmoprotectants proline and glycine betaine; expression in *E. coli* is induced by RpoS
249 and Fis on entry to stationary phase (53). Expression of *mysB*, *yahO,* and *yceK* are also RpoS-induced
250 (54). Expression of *katG* in *E. coli* was also shown to increase on entry into stationary phase, although
251 in an RpoS-independent manner (55).

252 Two genes with key roles in regulating entry into stationary phase entry in this group: *rsd* encodes an
253 anti-sigma factor that deactivates the exponential phase housekeeping sigma factor σ^{70} RpoD (56);
254 and *rmf* induces ribosome dimerization and hibernation (57). Expression of *rmf* is highly upregulated
255 in stationary phase in the SalComMac dataset (22). Both of these genes are upregulated far later in
256 the *acrB* mutant than in the wild type in our dataset; together with the other stationary-phase induced
257 genes in group three, this supports the later onset of stationary phase in Δ*acrB* than the wild type.

258 Expression of *aceB* is regulated by multiple transcription factors in *E. coli*, including ArcA (58). There
259 are also a number of genes in SPI-2, involved in intracellular survival, and chemotaxis-related genes in
260 group three.

261 Lower expression of SPI-2 genes were observed in other transcriptomics studies in the *acrB* D408A
262 mutant in exponential (6) and stationary phase (7), although the *met* genes and many others in group
263 three were not reflected in the datasets of previous studies. The reason for this is likely because most
264 genes in this group were transiently expressed in the wild type; we observed a "spike" of expression,
265 and later expression in the Δ*acrB* mutant. This reveals a key advantage of our approach; such a "spike"
266 could be missed if only a single timepoint was used to measure transcriptomes. Taking samples
267 through growth allows the expression of each gene to be tracked and the profiles of gene expression
268 over time to be compared.

269

270

271 ***A model linking efflux and stationary phase via membrane potential***

272 Previous studies have proposed that changes in gene expression and physiology in efflux knockouts
273 have been caused by the lack of efflux of a signalling molecule (for example an autoinducer), giving
274 rise to changes in intracellular and/or extracellular concentrations of that molecule and a resultant
275 change in gene regulation and physiology. However, we realised that knockout of *acrB* could trigger
276 an alternative signalling cascade. As AcrB requires proton motive force (PMF) for function,
277 deactivation of AcrB would decrease of influx of protons across the inner membrane, resulting in
278 membrane hyperpolarisation and thus alter the redox state of the cell. This has been built into a model
279 (Figure 3) whereby the membrane potential and redox state of the bacterium plays a key role in the
280 transition from exponential to stationary phase, mediated by the two-component ArcBA system (59).
281 Deletion of AcrB results in perturbation of the membrane potential and thereby the redox balance of
282 the cell and thus disrupts this regulation, resulting in a) late entry into stationary phase and b)
283 upregulation of anaerobic energy metabolism pathways.

284 The global regulator ArcBA regulates gene expression on the shift from aerobic to anaerobic
285 metabolism (59) and is also thought to play a role in response to other stresses such as reactive oxygen
286 species (ROS) and during infection in *Salmonella* (60, 61). Knockouts of *arcA* and *arcB* in *S.*
287 Typhimurium reduce intracellular survival in epithelial cells, macrophages and neutrophils, and are
288 attenuated in a mouse model (60). The ArcBA regulon has been characterised in *E. coli* (reviewed by
289 (59)) and *Salmonella* both aerobically and anaerobically (61, 62). The sensor kinase ArcB
290 autophosphorylates itself and then phosphorylates the response regulator ArcA; phospho-ArcA binds
291 promoter DNA and regulates gene expression (Figure 3a). Oxidised quinones repress the kinase
292 activity of ArcB (63) thus ArcBA is a direct sensor of the quinol pool redox state. Highly oxidised
293 quinone (Q) leads to low ArcA activity whereas highly reduced quinol (QH_2) leads to high ArcA activity.

294 ArcA has previously been shown to repress expression of *rpoS*, *rsd*, and *rmf*, three genes that mediate
295 important aspects of the switch from exponential phase to stationary phase (14, 64). RpoS is the sigma
296 factor that is dominant in stationary phase (14); *rpoS* transcription is repressed by ArcA in *E. coli* (65)
297 and *Salmonella* (66). In addition, activated ArcB phosphorylates RssB, which targets RpoS protein for
298 degradation by the ClpXP protease (65). ArcAB-RssB therefore acts as a key gatekeeper to entry into
299 stationary phase. Rsd is an anti-sigma factor that deactivates the exponential phase housekeeping
300 sigma factor σ^{70} / RpoD (56). Expression of *rsd* is regulated by ArcA in both *E. coli* (67) and *Salmonella*
301 (61). Rmf induces ribosome dimerization and hibernation in stationary phase (57); its expression is
302 ArcA-regulated in *Salmonella* (61) and *E. coli* (64).

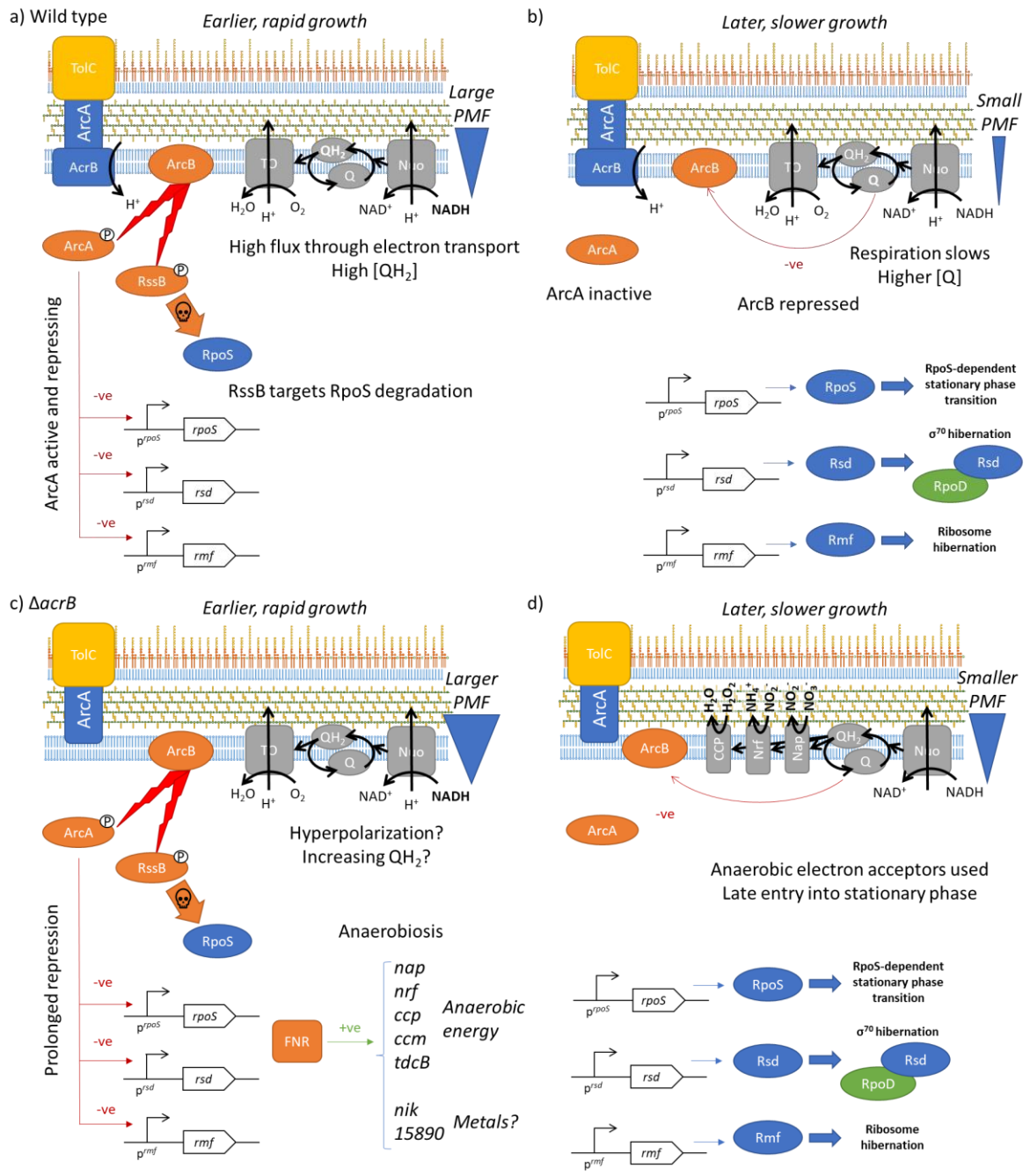

Figure 3. Model of the mechanism of ArcBA-mediated redox control of stationary phase entry and the impact of an AcrB mutant. In the wild type strain during rapid growth (a), high flux through the electron transport chain results in a reduced quinol pool (QH_2) which permits ArcBA to be active, repressing expression of *rpoS*, *rsd* and *rmf*. RssB also targets RpoS protein for degradation. As growth slows (b), the quinol pool becomes more oxidised (Q), deactivating ArcB, permitting activation of *rpoS*, *rsd* and *rmf*, triggering entry into stationary phase. In a *ΔacrB* mutant (c), proton motive force is higher for longer during growth, repressing *rpoS*, *rsd* and *rmf* and delaying entry into stationary phase. As a result, exponential phase physiology is extended (d), necessitating upregulation of genes involved in anaerobic energy metabolism (Nap, Nrf and CCP shown), likely via the global regulator FNR. TO: Terminal oxidases.

315 In the wild type in rapid growth, relatively high flux through electron transport to oxygen results in a
316 highly reduced quninol pool (QH_2). This would enable ArcBA to be active, repressing *rpoS*, *rsd* and *rmf*.
317 During entry into stationary phase, the quinol pool becomes more oxidised, de-activating ArcBA and
318 thus permitting *rpoS*, *rsd* and *rmf* expression and activity. In the transition of the *ΔacrB* strain to
319 stationary phase, the inner membrane would become hyperpolarised; this would alter the redox state
320 of the quinol pool, meaning that ArcBA remains active and RpoS, Rsd and Rmf activities are repressed
321 for longer during growth. This would delay onset of stationary phase in the Δ*acrB* mutant. The genes
322 *rsd* and *rmf* both fall into group three; Table 1 summarises their expression data. Expression of *rpoS* is
323 insignificant ($p_{adj} > 0.05$) in the wild type between 1 h and 3 h, although downregulated between 1 h
324 and 3 h in the Δ*acrB* mutant.

325

Log_2 fold change				**Δ*acrB* – wt Δlog_2**				
wt 1vs3	**wt 3vs5**	**acrB 1vs3**	**acrB 3vs5**	**1vs3**	**3vs5**	**ID**	**Gene**	**STM**
0.98	0.35†	-0.69	1.59	-1.67	1.24	SL1344_RS21380	*rsd*	STM4165
0.36†	0.73†	-1.17	2.19	-1.53	1.46	SL1344_RS15130	*rpoS*	STM2924
2.30	3.74	1.05	4.61	-1.25	0.87	SL1344_RS05235	*rmf*	STM1066

326

327 **Table 1. Gene expression data for the key stationary phase regulators *rsd*, *rmf*, and *rpoS*.** Log_2 fold change values for each
328 gene: 1 h vs 3 h in the wild type; 3 h vs 5 h in the wild type; 1 h vs 3 h in Δ*acrB*; 3 h vs 5 h in Δ*acrB*. ΔLog_2 values for the 1 h
329 vs 3 h and 3 h vs 5 h comparisons. Δlog_2 values are calculated by Log_2 fold change for Δ*acrB* minus Log_2 fold change for the
330 wild type. ID: locus name. Fold changes that are insignificant ($p_{adj} > 0.05$) are marked with a dagger †. Other fold changes are
331 colour coded as in Supplemental tables.

332

333 In the absence of a transition into stationary phase, exponential phase physiology would be prolonged
334 in the Δ*acrB* mutant with σ^{70} remaining the dominant sigma factor. Oxygen limitation caused by
335 increased biomass concentration would likely activate FNR, which would upregulate the anaerobic
336 energy-generating pathways identified in group two above. Nrf, Nap and CCP do not pump protons
337 across the inner membrane (68), therefore they would not contribute to the hyperpolarised state of
338 the bacterium. ArcA does not appear to regulate the anaerobically-activated genes identified here in
339 Supplemental Table S2 except for the periplasmic nitrite reductase *nrf* (62).

340

Experimental determination of membrane potential

To test whether the inner membrane of the Δ*acrB* strain is hyperpolarised, we used the fluorescent membrane potential dye $DiSC_3(5)$ (3,3'-dipropylthiadicarbocyanine iodide) (69). The wild type, Δ*acrB* and *acrB* D408A strains were grown in MOPS minimal medium and the membrane potential measured using flow cytometry after 1, 3 and 5 hours (Figure 4). As a control, the protonophore carbonyl cyanide m-chlorophenylhydrazone (CCCP) which collapses the PMF was used prior to measurement. The wild type strain showed highest membrane potential after 1 hours growth, and declining membrane potential at 3 and 5 hours. Both the Δ*acrB* strain and a strain expressing the *acrB* D408A derivative, which blocks proton translocation and thus efflux (70, 71), had higher membrane potential than the wild type at all time points. These data support the hypothesis that the Δ*acrB* mutant is hyperpolarised. Treatment with CCCP collapsed the membrane potential of all strains at all time points ($P \leq 0.01$).

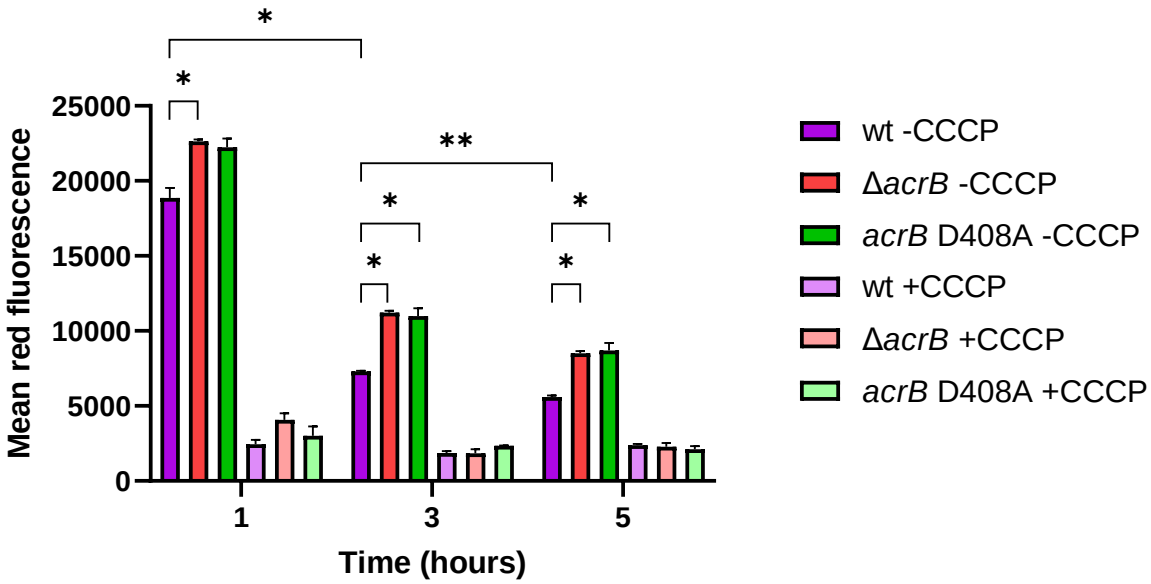

Figure 4. Determination of membrane potential. SL1344, Δ*acrB* and *acrB* D408A cells were grown in MOPS minimal medium and samples taken at 1, 3 and 5 hours growth, whereupon membrane potential was determined using flow cytometry and $DiSC_3(5)$. The red fluorescence, corresponding to membrane potential, is shown for each strain. The protonophore CCCP was used as a control to collapse membrane potential. Error bars show standard deviation of duplicate cultures for a representative experiment. Significance was tested for comparisons of wild type and Δ*acrB* / *acrB* D408A strains for each timepoint and across timepoints using a paired t-test; * $P \leq 0.05$; ** $P \leq 0.01$. Addition of CCCP to each sample resulted in a significant ($P \leq 0.01$) decrease in membrane potential.

There is only one other study where the influence of efflux pumps on membrane potential has been measured; Le *et al*. showed that PMF was similar in wt and *tolC* strains of *E. coli* by measuring flagellar

365 rotor speed (72). These experiments were done on cells grown in rich medium to an optical density of
366 2, so are not directly comparable with our data.

367 **Discussion**

368 Our transcriptomics data suggests that the Δ*acrB* strain enters stationary phase later than the wild
369 type, and as a result displays prolonged exponential-phase anaerobic metabolism. Comparison with
370 other transcriptomic experiments on efflux pump mutants reveals some similarities in expression
371 patterns. Wang-Kan *et al*. compared expression in SL1344 and an efflux-defective *acrB* D408A mutant
372 (6). The two strains were grown in MOPS minimal medium to an OD_{600} of 0.6. The *acrB* D408A mutant
373 displayed higher expression of flagella and anaerobic metabolism genes than the wild type. A later
374 transcriptomic study (7) grew the same strains in LB broth to stationary phase and found changes in
375 genes responsible for energy metabolism. A major advantage of measuring gene expression across
376 growth (here at 1, 3 and 5 hours) is that trends in gene expression (and thereby physiology) over time
377 can be identified, which would otherwise be difficult to detect or interpret when taking samples at
378 only a single timepoint.

379 ***Supporting evidence for the redox-ArcBA model from the literature***

380 There is data in the literature to support the model of efflux pump function influencing membrane
381 potential and regulation of stationary phase (Fig. 3). The links between efflux pumps and membrane
382 potential have previously been observed in studies on efflux pump inhibitors. The antihistamine
383 promethazine (a phenothiazine) is an efflux pump inhibitor (73) and has been shown to increase
384 membrane potential in *Pseudomonas aeruginosa* (74).

385 Arce-Rodríguez *et al*. studied the impact of the $NADH:NAD^+$ ratio on antibiotic resistance in
386 *Pseudomonas aeruginosa* PA14 (75). They artificially modulated the $NADH:NAD^+$ ratio using a
387 recombinant NADH oxidase (which increases $[NAD^+]$) or a formate dehydrogenase (which increases
388 [NADH]). They showed that a high $NADH:NAD^+$ ratio increased membrane potential whereas low
389 $NADH:NAD^+$ ratios decreased membrane potential (measured using $DiOC_2(3)$). High $NADH:NAD^+$ ratios
390 also increased cellular ROS levels, and efflux of aminoglycosides and fluoroquinolones via the RND
391 efflux pumps MexAB and MexXY leading to increased resistance. However, a high $NADH:NAD^+$ ratio
392 also increased ROS-mediated killing by high concentrations of antibiotics, and it was concluded that
393 control of $NADH:NAD^+$ ratio and other aspects of redox balance was important for response to
394 antibiotics.

395 Yang *et al*. found that an Δ*acrA* mutant in *E. coli* BW25113 had lower *rpoS::lacZ* expression than the
396 wild type across growth, while overproduction of AcrA resulted in increased *rpoS::lacZ* expression (76).

397 Yang *et al*. proposed that efflux pumps export quorum sensing molecules which gives rise to these
398 changes in physiology, but we present an alternative model whereby membrane potential and redox
399 state is the signal. Indeed, subsequent studies have sought to identify effluxed quorum sensing
400 molecules without success (7). A previous study found that *rpoS* transcription in *S.* Typhimurium F98
401 is linked to redox and influenced by oxygen, ArcA, and NADH:NAD^+ ratio (66). Expression of *arcA* was
402 also found to be negatively regulated by RpoS. The authors also suggested that quorum sensing could
403 play a role in this regulation. ArcA has also recently been found to be important in *E. coli* for
404 development of antibiotic resistance (77) and metabolic adaptation to tetracycline resistance (78).

405 ***Links to biofilms?***

406 It has previously been reported that knockout or deactivation of *acrB* and other genes encoding efflux
407 pump components reduced biofilm formation in *Salmonella* (79), although the exact regulatory
408 mechanism is currently unclear (80, 81) . Indeed, efflux pumps have been implicated in biofilm
409 formation in many bacterial species (reviewed by (82)). A recent study identified TolC as being
410 beneficial for biofilm formation in both *E. coli* and *S*. Typhimurium (81). This study also identified *nuo*
411 genes encoding the major aerobic NADH reductase as being important in *Salmonella* biofilm
412 formation, and highlighted the fact that biofilm development is a process requiring different genes at
413 different times (from initial attachment to maturation). Efflux inhibitors such as phenothiazines have
414 also been shown to reduce biofilm formation (73, 74). ArcBA and RpoS have previously been
415 implicated in regulation of biofilm formation (83) so our model could provide a link between efflux
416 pumps, redox state, and biofilm formation. Indeed, recent studies have shown that *Salmonella* biofilm
417 formation can be modulated by redox-active polymers (84).

418

419 **Conclusions**

420 In summary, we have demonstrated that deactivation of AcrB leads to hyperpolarisation of the inner
421 membrane and we propose that this is responsible for wide-ranging changes in bacterial gene
422 regulation and physiology. Our model linking efflux and redox provides an explanation for some
423 phenotypes observed in efflux pump knockouts and inhibition experiments, and places efflux pumps
424 as a central part of bacterial physiology, distinct from (but linked to) their role as transporters of
425 noxious substances from the cell.

426 Intriguingly, our model could explain three reasons why efflux pumps are important for the response
427 of *Salmonella* to antimicrobials. First, their well-established and characterised function in removing
428 noxious substances from the cell. Second, as loss of AcrB function increases membrane potential,

429 antimicrobials postulated to function via the generation of reactive oxygen species by the respiratory
430 chain following treatment (the ROS-lethality hypothesis) (85) could be more effective. And third, as
431 the Δ*acrB* strain appears to enter stationary phase later in growth than the wild type, inhibition of
432 efflux is likely to delay the remodelling of the cell envelope that occurs on transition to stationary
433 phase, after which antimicrobial permeability is far reduced (9). Likewise, the attenuation of virulence
434 observed when AcrB is deactivated (6) could be due to deficiencies in efflux of antimicrobial host
435 molecules, and / or changes in physiology brought about by hyperpolarisation such as alterations in
436 SPI expression, motility, and biofilm formation. Future work will explore the relative contributions of
437 efflux and redox state in these situations.

438

439 **Materials and Methods**

440 *Salmonella enterica* serovar Typhimurium SL1344 (86) and its cognate Δ*acrB* (87) and *acrB* D408A
441 mutant (6) were used. Transcriptomic analysis on SL1344 and SL1344 Δ*acrB* was performed as
442 described by (9). RNA-Seq data have been deposited with Array Express (accession no. E-MTAB-9679).

443 Total numbers of differentially expressed genes (DEGs) were determined using the R package DESeq2
444 (88) by comparing the three timepoints (1h, 3h, and 5h) for both the wild type and the Δ*acrB* strain.
445 Adjusted p-value < 0.05 and $\log_2$FC ≥ |1.5| were both used as the thresholds for determining the DEGs
446 for the Venn diagrams (Figure 1), which were drawn using the R package ggvenn (89).

447 Genes were classified in groups 1, 2 and 3 by the following criteria. The $\log_2$ fold change for each gene
448 was calculated for 1 h versus 3 h in both wt and Δ*acrB* strains. Only genes where $\log_2$FC data were
449 significant (p_{adj} < 0.05) for the 1 h vs 3 h comparison for both wt and Δ*acrB* strains were considered
450 for this analysis. Δ$\log_2$FC was calculated for each gene by subtracting the $\log_2$FC in the wt from the
451 $\log_2$FC in the Δ*acrB* strain. Groups were classified: group 1, wt $\log_2$FC for 1 h vs 3 h was ≤ -1 and Δ$\log_2$FC
452 was ≥ 1; Group 2, wt $\log_2$FC for 1 h vs 3 h was > -1 and Δ$\log_2$FC was ≥ 1; Group 3, Δ$\log_2$FC was ≤ 1.

453 **Membrane potential measurement by flow cytometry**

454 Strains SL1344, Δ*acrB* and *arcB* D408A were grown in 10 mL of MOPS minimal medium (9) at 37 °C.
455 After 1, 3 and 5 hours, cells were harvested by centrifugation (4720 x g for 5 min) and resuspended in
456 filter-sterilised HEPES-buffered saline (HBS, Alfa Aesar). Diluted cell suspensions were added to tubes
457 containing HBS. 15 µM CCCP was added to control samples and incubated for 15 min with shaking in
458 the dark. To all samples was added 1 µM $DiSC_3(5)$, 1% DMSO, 0.2% Glucose, and 1 mM $CaCl_2$ before
459 being shaken for a further 15 min in the dark (69). Samples were then analysed using a C6 Plus flow
460 cytometer (BD Biosciences) and CFlow plus software. Data rate was 1000 to 4000 events/sec and a

461 FSC-H threshold of 8000 was used to discriminate noise from bacteria. Bacteria were gated using
462 forward scatter and side scatter measurements from blue laser illumination (488 nm), and red
463 fluorescence was measured using red laser illumination (640 nm) and collected using a 670 LP filter.

464 **Acknowledgements**

465 ***Conflicts of interest:*** We declare that the research was conducted in the absence of any commercial
466 or financial relationships that might be considered a conflict of interest.

467 ***Author contributions:*** J.M.A.B., T.W.O., and E.E.W. designed the assays. E.E.W. performed
468 experiments to obtain samples for RNA-seq. A.O. and S.J.E. performed experiments to measure
469 membrane potential and analysed the resulting data. RNA-seq data were analyzed by E.E.W., O.O.,
470 and T.W.O. The manuscript was written by J.M.A.B. and T.W.O. with input from all authors.

471 ***Funding:*** E.E.W. was funded by AAMR Wellcome Trust DTP grant 108876/B/15/Z at the University of
472 Birmingham. O.O. was funded by a UK Biotechnology & Biological Sciences Research Council (BBSRC)
473 PhD studentship through the Midlands Integrative Biosciences Training Partnership (MIBTP) scheme.
474 S.J.E. was funded by a Centre for Systems Modelling and Quantitative Biomedicine (SMQB), University
475 of Birmingham grant to J.M.A.B. A.O. was funded by a University of Birmingham Institute of Global
476 Innovation / Institute of Advanced Studies grant to T.W.O. and J.M.A.B. J.M.A.B. was funded by BBSRC
477 grant BB/M02623X/1 (David Phillips Fellowship to J.M.A.B.).

478 The authors would like to thank Xuan Wang-Kan and Laura Piddock for sharing data from previous
479 studies, and Henrik Strahl for discussions on membrane potential measurement.

480 **References**

481 1. Darby EM, Trampari E, Siasat P, Gaya MS, Alav I, Webber MA, Blair JMA. 2023. Molecular
482 mechanisms of antibiotic resistance revisited. Nat Rev Microbiol 21:280–295.

483 2. Blair JMA, Richmond GE, Piddock LJV. 2014. Multidrug efflux pumps in Gram-negative bacteria
484 and their role in antibiotic resistance. Future Microbiol 9:1165–1177.

485 3. Nikaido H. 1989. Outer membrane barrier as a mechanism of antimicrobial resistance.
486 Antimicrob Agents Chemother 33:1831–1836.

487 4. Colclough AL, Alav I, Whittle EE, Pugh HL, Darby EM, Legood SW, McNeil HE, Blair JMA. 2020.
488 RND efflux pumps in Gram-negative bacteria; Regulation, structure and role in antibiotic
489 resistance. Future Microbiol 15:143-157.

490 5. Webber MA, Bailey AM, Blair JMA, Morgan E, Stevens MP, Hinton JCD, Ivens A, Wain J, Piddock
491 LJV. 2009. The global consequence of disruption of the AcrAB-TolC efflux pump in *Salmonella*
492 *enterica* includes reduced expression of SPI-1 and other attributes required to infect the host. J
493 Bacteriol 191:4276–4285.

494 6. Wang-Kan X, Blair JMA, Chirullo B, Betts J, La Ragione RM, Ivens A, Ricci V, Opperman TJ,
495 Piddock LJV. 2017. Lack of AcrB efflux function confers loss of virulence on *Salmonella enterica*
496 serovar Typhimurium. mBio 8:e00968-17.

497 7. Wang-Kan X, Rodríguez-Blanco G, Southam AD, Winder CL, Dunn WB, Ivens A, Piddock LJV.
498 2021. Metabolomics reveal potential natural substrates of AcrB in *Escherichia coli* and
499 *Salmonella enterica* serovar Typhimurium. mBio 12:e00109-21.

500 8. Buckner MMC, Blair JMA, La Ragione RM, Newcombe J, Dwyer DJ, Ivens A, Piddock LJV. 2016.
501 Beyond antimicrobial resistance: Evidence for a distinct role of the AcrD efflux pump in
502 *Salmonella* biology. mBio 7:e01916-16.

503 9. Whittle EE, McNeil HE, Trampari E, Webber M, Overton TW, Blair JMA. 2021. Efflux Impacts
504 Intracellular Accumulation Only in Actively Growing Bacterial Cells. mBio 12:e0260821.

505 10. Leus I V., Adamiak J, Chandar B, Bonifay V, Zhao S, Walker SS, Squadroni B, Balibar CJ, Kinarivala
506 N, Standke LC, Voss HU, Tan DS, Rybenkov V V., Zgurskaya HI. 2023. Functional Diversity of
507 Gram-Negative Permeability Barriers Reflected in Antibacterial Activities and Intracellular
508 Accumulation of Antibiotics. Antimicrob Agents Chemother 67:e01377-22.

509 11. Manrique PD, López CA, Gnanakaran S, Rybenkov V V., Zgurskaya HI. 2023. New understanding
510 of multidrug efflux and permeation in antibiotic resistance, persistence, and heteroresistance.
511 Ann N Y Acad Sci 1519:46–62.

512 12. Li J, Claudi B, Fanous J, Chicherova N, Cianfanelli FR, Campbell RAA, Bumann D. 2021. Tissue
513 compartmentalization enables *Salmonella* persistence during chemotherapy. Proc Natl Acad Sci
514 U S A 118:e2113951118.

515 13. Łapińska U, Voliotis M, Lee KK, Campey A, Stone RML, Tuck B, Phetsang W, Zhang B, Tsaneva-
516 Atanasova K, Blaskovich MAT, Pagliara S. 2022. Fast bacterial growth reduces antibiotic
517 accumulation and efficacy. elife 11:e74062.

518 14. Navarro Llorens JM, Tormo A, Martínez-García E. 2010. Stationary phase in Gram-negative
519 bacteria. FEMS Microbiol Rev 34:476–495.

520 15. Battesti A, Majdalani N, Gottesman S. 2011. The RpoS-mediated general stress response in
521 *Escherichia coli*. Annu Rev Microbiol 65:189–213.

522 16. Durfee T, Hansen AM, Zhi H, Blattner FR, Ding JJ. 2008. Transcription profiling of the stringent
523 response in *Escherichia coli*. J Bacteriol 190:1084–1096.

524 17. Singh SK, Saisree L, Amrutha RN, Reddy M. 2012. Three redundant murein endopeptidases
525 catalyse an essential cleavage step in peptidoglycan synthesis of *Escherichia coli* K12. Mol
526 Microbiol 86:1036–1051.

527 18. Harmon DE, Ruiz C. 2022. The Multidrug Efflux Regulator AcrR of *Escherichia coli* Responds to
528 Exogenous and Endogenous Ligands To Regulate Efflux and Detoxification. mSphere 7:e00474-
529 22.

530 19. Lou L, Zhang P, Piao R, Wang Y. 2019. *Salmonella* Pathogenicity Island 1 (SPI-1) and Its Complex
531 Regulatory Network. Front Cell Infect Microbiol 9:270.

532 20. Sánchez-Romero MA, Casadesús J. 2018. Contribution of SPI-1 bistability to *Salmonella enterica*
533 cooperative virulence: insights from single cell analysis. Sci Rep 8:14875.

534 21. Ilyas B, Tsai CN, Coombes BK. 2017. Evolution of *Salmonella*-host cell interactions through a
535 dynamic bacterial genome. Front Cell Infect Microbiol 7:428.

536 22. Kröger C, Colgan A, Srikumar S, Händler K, Sivasankaran SK, Hammarlöf DL, Canals R, Grissom JE,
537 Conway T, Hokamp K, Hinton JCD. 2013. An infection-relevant transcriptomic compendium for
538 *Salmonella enterica* serovar Typhimurium. Cell Host Microbe 14:683–695.

539 23. Srikumar S, Kröger C, Hébrard M, Colgan A, Owen S V., Sivasankaran SK, Cameron ADS, Hokamp
540 K, Hinton JCD. 2015. RNA-seq Brings New Insights to the Intra-Macrophage Transcriptome of
541 *Salmonella* Typhimurium. PLoS Pathog 11:e1005262.

542 24. Hoiseth SK, Stocker BAD. 1981. Aromatic-dependent *Salmonella* Typhimurium are non-virulent
543 and effective as live vaccines. Nature 291:238–239.

544 25. Fink RC, Evans MR, Porwollik S, Vazquez-Torres A, Jones-Carson J, Troxell B, Libby SJ, McClelland
545 M, Hassan HM. 2007. FNR is a global regulator of virulence and anaerobic metabolism in
546 *Salmonella enterica* serovar Typhimurium (ATCC 14028s). J Bacteriol 189:2262–2273.

547 26. Constantinidou C, Hobman JL, Griffiths L, Patel MD, Penn CW, Cole JA, Overton TW. 2006. A
548 reassessment of the FNR regulon and transcriptomic analysis of the effects of nitrate, nitrite,
549 NarXL, and NarQP as *Escherichia coli* K12 adapts from aerobic to anaerobic growth. J Biol Chem
550 281:4802–4815.

551 27. Nilavongse A, Brondijk THC, Overton TW, Richardson DJ, Leach ER, Cole JA. 2006. The NapF
552 protein of the *Escherichia coli* periplasmic nitrate reductase system: Demonstration of a
553 cytoplasmic location and interaction with the catalytic subunit, NapA. Microbiology 152:3227–
554 3237.

555 28. Browning DF, Grainger DC, Beatty CM, Wolfe AJ, Cole JA, Busby SJW. 2005. Integration of three
556 signals at the *Escherichia coli nrf* promoter: A role for Fis protein in catabolite repression. Mol
557 Microbiol 57:496–510.

558 29. Kim MJ, Lim S, Ryu S. 2008. Molecular analysis of the *Salmonella* Typhimurium *tdc* operon
559 regulation. J Microbiol Biotechnol 18:1024–1032.

560 30. Cianciotto NP, Cornelis P, Baysse C. 2005. Impact of the bacterial type I cytochrome *c*
561 maturation system on different biological processes. Mol Microbiol 56:1408–1415.

562 31. Khademian M, Imlay JA. 2017. *Escherichia coli* cytochrome *c* peroxidase is a respiratory oxidase
563 that enables the use of hydrogen peroxide as a terminal electron acceptor. Proc Natl Acad Sci U
564 S A 114:E6922–E6931.

565 32. Pelosi L, Vo CDT, Abby SS, Loiseau L, Rascalou B, Chehade MH, Faivre B, Goussé M, Chenal C,
566 Touati N, Binet L, Cornu D, Fyfe CD, Fontecave M, Barras F, Lombard M, Pierrel F. 2019.
567 Ubiquinone biosynthesis over the entire O_2 range: Characterization of a conserved O_2-
568 independent pathway. mBio 10:e01319-19.

569 33. Navarro C, Wu L -F, Mandrand-Berthelot M -A. 1993. The *nik* operon of *Escherichia coli* encodes
570 a periplasmic binding-protein-dependent transport system for nickel. Mol Microbiol 9:1181–
571 1191.

572 34. Rowe JL, Starnes GL, Chivers PT. 2005. Complex transcriptional control links NikABCDE-
573 dependent nickel transport with hydrogenase expression in *Escherichia coli*. J Bacteriol
574 187:6317–6323.

575 35. Piotrowska AA. 2018. Investigation of STM3071 as a potential regulator of cobalt transport in
576 *Salmonella enterica*. PhD thesis. Edinburgh Napier University, UK.

577 36. Karavolos MH, Spencer H, Bulmer DM, Thompson A, Winzer K, Williams P, Hinton JCD, Khan
578 CMA. 2008. Adrenaline modulates the global transcriptional profile of *Salmonella* revealing a
579 role in the antimicrobial peptide and oxidative stress resistance responses. BMC Genomics
580 9:458.

581 37. Wood MW, Jones MA, Watson PR, Hedges S, Wallis TS, Galyov EE. 1998. Identification of a
582 pathogenicity island required for *Salmonella* enteropathogenicity. Mol Microbiol 29:883–891.

583 38. Cohen H, Adani B, Cohen E, Piscon B, Azriel S, Desai P, Bähre H, McClelland M, Rahav G, Gal-Mor
584 O. 2022. The ancestral stringent response potentiator, DksA has been adapted throughout
585 *Salmonella* evolution to orchestrate the expression of metabolic, motility, and virulence
586 pathways. Gut Microbes 14:1997294.

587 39. Frye J, Karlinsey JE, Felise HR, Marzolf B, Dowidar N, McClelland M, Hughes KT. 2006.
588 Identification of new flagellar genes of *Salmonella enterica* serovar Typhimurium. J Bacteriol
589 188:2233–2243.

590 40. Hamed S, Wang X, Shawky RM, Emara M, Aldridge PD, Rao C V. 2019. Synergistic action of SPI-1
591 gene expression in *Salmonella enterica* serovar Typhimurium through transcriptional crosstalk
592 with the flagellar system. BMC Microbiol 19:211.

593 41. Liu R, Blackwell TW, States DJ. 2001. Conformational model for binding site recognition by the *E.*
594 *coli* MetJ transcription factor. Bioinformatics 17:622–633.

595 42. Grogan DW, Cronan JE. 1997. Cyclopropane ring formation in membrane lipids of bacteria.
596 Microbiol Mol Biol Rev 61:429–441.

597 43. Wei Y, Newman EB. 2002. Studies on the role of the *metK* gene product of *Escherichia coli* K-12.
598 Mol Microbiol 43:1651–1656.

599 44. Newman EB, Budman LI, Chan EC, Greene RC, Lin RT, Woldringh CL, D'ari R. 1998. Lack of S-
600 adenosylmethionine results in a cell division defect in *Escherichia coli*. J Bacteriol 180:3614–
601 3619.

602 45. Husna AU, Wang N, Cobbold SA, Newton HJ, Hocking DM, Wilksch JJ, Scott TA, Davies MR,
603 Hinton JC, Tree JJ, Lithgow T, McConville MJ, Strugnell RA. 2018. Methionine biosynthesis and
604 transport are functionally redundant for the growth and virulence of *Salmonella* Typhimurium. J
605 Biol Chem 293:9506–9519.

606 46. Zimbro MJ, Power DA, Miller SM, Wilson GE, Johnson JA. 2009. Difco and BBL Manual.

607 47. Dolzan M, Johansson K, Roig-Zamboni V, Campanacci V, Tegoni M, Schneider G, Cambillau C.
608 2004. Crystal structure and reactivity of YbdL from *Escherichia coli* identify a methionine
609 aminotransferase function. FEBS Lett 571:141–146.

610 48. Heilbronn J, Wilson J, Berger BJ. 1999. Tyrosine aminotransferase catalyzes the final step of
611 methionine recycling in *Klebsiella pneumoniae*. J Bacteriol 181:1739–1747.

612 49. Sévin DC, Fuhrer T, Zamboni N, Sauer U. 2017. Nontargeted in vitro metabolomics for high-
613 throughput identification of novel enzymes in *Escherichia coli*. Nat Methods 14:187–194.

614 50. Hwang S, Choe D, Yoo M, Cho S, Kim SC, Cho S, Cho BK. 2018. Peptide transporter CstA imports
615 pyruvate in *Escherichia coli* K-12. J Bacteriol 200:e00771-17.

616 51. McDermott JE, Yoon H, Nakayasu ES, Metz TO, Hyduke DR, Kidwai AS, Palsson BO, Adkins JN,
617 Heffron F. 2011. Technologies and approaches to elucidate and model the virulence program of
618 *Salmonella*. Front Microbiol 2:121.

619 52. Taschner NP, Yagil E, Spira B. 2004. A differential effect of σ^s on the expression of the Pho
620 regulon genes of *Escherichia coli*. Microbiology 150:2985–2992.

621 53. Typas A, Stella S, Johnson RC, Hengge R. 2007. The -35 sequence location and the Fis-sigma
622 factor interface determine σ^S selectivity of the *proP* (P2) promoter in *Escherichia coli*. Mol
623 Microbiol 63:780–796.

624 54. Weber H, Polen T, Heuveling J, Wendisch VF, Hengge R. 2005. Genome-wide analysis of the
625 general stress response network in *Escherichia coli*: σ^S-dependent genes, promoters, and sigma
626 factor selectivity. J Bacteriol 187:1591–1603.

627 55. Mukhopadhyay S, Schellhorn HE. 1994. Induction of *Escherichia coli* hydroperoxidase I by
628 acetate and other weak acids. J Bacteriol 176:2300–2307.

629 56. Piper SE, Mitchell JE, Lee DJ, Busby SJW. 2009. A global view of *Escherichia coli* Rsd protein and
630 its interactions. Mol Biosyst 5:1943–1947.

631 57. Starosta AL, Lassak J, Jung K, Wilson DN. 2014. The bacterial translation stress response. FEMS
632 Microbiol Rev 38:1172–1201.

633 58. Waegeman H, Beauprez J, Moens H, Maertens J, De Mey M, Foulquié-Moreno MR, Heijnen JJ,
634 Charlier D, Soetaert W. 2011. Effect of *iclR* and *arcA* knockouts on biomass formation and
635 metabolic fluxes in *Escherichia coli* K-12 and its implications on understanding the metabolism
636 of *Escherichia coli* BL21 (DE3). BMC Microbiol 11:70.

637 59. Brown AN, Anderson MT, Bachman MA, Mobley HLT. 2022. The ArcAB Two-Component System:
638 Function in Metabolism, Redox Control, and Infection. Microbiol Mol Biol Rev 86:e0011021.

639 60. Pardo-Esté C, Hidalgo AA, Aguirre C, Briones AC, Cabezas CE, Castro-Severyn J, Fuentes JA,
640 Opazo CM, Riedel CA, Otero C, Pacheco R, Valvano MA, Saavedra CP. 2018. The ArcAB two-
641 component regulatory system promotes resistance to reactive oxygen species and systemic
642 infection by *Salmonella* Typhimurium. PLoS One 13:e0203497.

643 61. Morales EH, Collao B, Desai PT, Calderón IL, Gil F, Luraschi R, Porwollik S, McClelland M,
644 Saavedra CP. 2013. Probing the ArcA regulon under aerobic/ROS conditions in *Salmonella*
645 *enterica* serovar Typhimurium. BMC Genomics 14:626.

646 62. Evans MR, Fink RC, Vazquez-Torres A, Porwollik S, Jones-Carson J, McClelland M, Hassan HM.
647 2011. Analysis of the ArcA regulon in anaerobically grown *Salmonella enterica* sv. Typhimurium.
648 BMC Microbiol 11:58.

649 63. Sharma P, Stagge S, Bekker M, Bettenbrock K, Hellingwerf KJ. 2013. Kinase Activity of ArcB from
650 *Escherichia coli* Is Subject to Regulation by Both Ubiquinone and Demethylmenaquinone. PLoS
651 One 8:e75412.

652 64. Yoshida H, Wada A, Shimada T, Maki Y, Ishihama A. 2019. Coordinated Regulation of Rsd and
653 RMF for Simultaneous Hibernation of Transcription Apparatus and Translation Machinery in
654 Stationary-Phase *Escherichia coli*. Front Genet 10:1153.

655 65. Mika F, Hengge R. 2005. A two-component phosphotransfer network involving ArcB, ArcA, and
656 RssB coordinates synthesis and proteolysis of σ^S (RpoS) in *E. coli*. Genes Dev 19:2770–2781.

657 66. Ševčík M, Šebková A, Volf J, Rychlík I. 2001. Transcription of *arcA* and *rpoS* during growth of
658 *Salmonella* Typhimurium under aerobic and microaerobic conditions. Microbiology 147:701–
659 708.

660 67. Park DM, Akhtar MS, Ansari AZ, Landick R, Kiley PJ. 2013. The Bacterial Response Regulator ArcA
661 Uses a Diverse Binding Site Architecture to Regulate Carbon Oxidation Globally. PLoS Genet
662 9:e1003839.

663 68. Simon J, van Spanning RJM, Richardson DJ. 2008. The organisation of proton motive and non-
664 proton motive redox loops in prokaryotic respiratory systems. Biochim Biophys Acta - Bioenerg
665 1777:1480–1490.

666 69. Buttress JA, Halte M, Derkte Winkel J, Erhardt M, Popp PF, Strahl H. 2022. A guide for
667 membrane potential measurements in Gram-negative bacteria using voltage-sensitive dyes.
668 Microbiol (United Kingdom) 168:001227.

669 70. Seeger MA, Von Ballmoos C, Verrey F, Pos KM. 2009. Crucial role of Asp408 in the proton
670 translocation pathway of multidrug transporter AcrB: Evidence from site-directed mutagenesis
671 and carbodiimide labeling. Biochemistry 48:5801–5812.

672 71. Su CC, Li M, Gu R, Takatsuka Y, McDermott G, Nikaido H, Yu EW. 2006. Conformation of the
673 AcrB multidrug efflux pump in mutants of the putative proton relay pathway. J Bacteriol
674 188:7290–7296.

675 72. Le D, Krasnopeeva E, Sinjab F, Pilizota T, Kim M. 2021. Active efflux leads to heterogeneous
676 dissipation of proton motive force by protonophores in bacteria. mBio 12:e0067621.

677 73. Grimsey EM, Piddock LJV. 2019. Do phenothiazines possess antimicrobial and efflux inhibitory
678 properties? FEMS Microbiol Rev 43:577–590.

679 74. Donnert M, Elsheikh S, Arce-Rodriguez A, Pawar V, Braubach P, Jonigk D, Haverich A, Weiss S,
680 Müsken M, Häussler S. 2020. Targeting bioenergetics is key to counteracting the drug-tolerant
681 state of biofilm-grown bacteria. PLoS Pathog 16:e1009126.

682 75. Arce-Rodríguez A, Pankratz D, Preusse M, Nikel PI, Häussler S. 2022. Dual Effect: High NADH
683 Levels Contribute to Efflux-Mediated Antibiotic Resistance but Drive Lethality Mediated by
684 Reactive Oxygen Species. mBio 13:e0243421.

685 76. Yang S, Lopez CR, Zechiedrich EL. 2006. Quorum sensing and multidrug transporters in
686 *Escherichia coli.* Proc Natl Acad Sci U S A 103:2386–2391.

687 77. Horinouchi T, Maeda T, Kotani H, Furusawa C. 2020. Suppression of antibiotic resistance
688 evolution by single-gene deletion. Sci Rep 10:4178.

689 78. Arrieta-Ortiz ML, Pan M, Kaur A, Pepper-Tunick E, Srinivas V, Dash A, Immanuel SRC, Brooks AN,
690 Shepherd TR, Baliga NS. 2023. Disrupting the ArcA Regulatory Network Amplifies the Fitness
691 Cost of Tetracycline Resistance in *Escherichia coli*. mSystems 8:e00904-22.

692 79. Baugh S, Ekanayaka AS, Piddock LJV, Webber MA. 2012. Loss of or inhibition of all multidrug
693 resistance efflux pumps of *Salmonella enterica* serovar Typhimurium results in impaired ability
694 to form a biofilm. J Antimicrob Chemother 67:2409–2417.

695 80. Holden ER, Webber MA. 2020. MarA, RamA, and SoxS as Mediators of the Stress Response:
696 Survival at a Cost. Front Microbiol 11:828.

697 81. Holden ER, Yasir M, Turner AK, Charles IG, Webber MA. 2022. Comparison of the genetic basis
698 of biofilm formation between *Salmonella* Typhimurium and *Escherichia coli*. Microb Genomics
699 8:000885.

700 82. Alav I, Sutton JM, Rahman KM. 2018. Role of bacterial efflux pumps in biofilm formation. J
701 Antimicrob Chemother 73:2003–2020.

702 83. Hengge R. 2008. The two-component network and the general stress sigma factor RpoS (σ^S) in
703 *Escherichia coli*. Adv Exp Med Biol 631:40–53.

704 84. Gomez-Carretero S, Libberton B, Svennersten K, Persson K, Jager E, Berggren M, Rhen M,
705 Richter-Dahlfors A. 2017. Redox-active conducting polymers modulate *Salmonella* biofilm
706 formation by controlling availability of electron acceptors. npj Biofilms Microbiomes 3:19.

707 85. Kohanski MA, Dwyer DJ, Hayete B, Lawrence CA, Collins JJ. 2007. A Common Mechanism of
708 Cellular Death Induced by Bactericidal Antibiotics. Cell 130:797–810.

709 86. Brenner FW, Villar RG, Angulo FJ, Tauxe R, Swaminathan B. 2000. *Salmonella* nomenclature. J
710 Clin Microbiol 38:2465–2467.

711 87. Eaves DJ, Ricci V, Piddock LJV. 2004. Expression of *acrB, acrF, acrD, marA,* and *soxS* in
712 *Salmonella enterica* Serovar Typhimurium: Role in Multiple Antibiotic Resistance. Antimicrob
713 Agents Chemother 48:1145–1150.

714 88. Love MI, Huber W, Anders S. 2014. Moderated estimation of fold change and dispersion for
715 RNA-seq data with DESeq2. Genome Biol 15:550.

716 89. Gao CH, Yu G, Cai P. 2021. ggVennDiagram: An Intuitive, Easy-to-Use, and Highly Customizable R
717 Package to Generate Venn Diagram. Front Genet 12:706907.

718 90. Whittle EE, Legood SW, Alav I, Dulyayangkul P, Overton TW, Blair JMA. 2019. Flow Cytometric
719 Analysis of Efflux by Dye Accumulation. Front Microbiol 10:2319.

720